

Garment Plotter Based on ARM Embedded System

Khadijah Mansour*

University of Garden City, Sudan

**corresponding author*

Keywords: Arm Embedded System, Clothing Plotter, Mercator Projection Algorithm, Escape Time Algorithm

Abstract: In recent years, with the advancement of chip production technology and the continuous optimization of image processing, digital image processing technology has made great progress in many fields such as communications, medical care, meteorology, navigation, aerospace, intelligent transportation, applications, etc. Great progress has been made. This article aims to integrate embedded development, clothing drawing, system testing and other technologies, analyze the shortcomings and shortcomings of the existing plotting station terminal, propose a terminal upgrade plan according to the design requirements and indicators of the system, and analyze the terminal hardware and software system platform in detail Build and realize the process of Qt application program, so as to improve the rapidity and intelligent level of the plotting platform system. Combining the design requirements and performance indicators of the system, the hardware and software design schemes of the terminal are respectively given, and the Qt Designer development tool and the unique signal and slot mechanism are briefly introduced. Secondly, introduce the theoretical basis involved in the terminal design process of the plotting station: detailed analysis of the coordinate transformation formulas of Mercator and Gaussian projections, the calculation formulas of clothing deformation correction; comparison of several commonly used path planning algorithms, select AI algorithm for path planning Plan and use Matlab to simulate and verify the performance of the algorithm. The innovation of this article is based on the high-performance ARM processor and embedded ARM operating system, and makes full use of the cross-platform features of the Qt platform. The experimental results show that compared with the existing plotting station terminal, it has good human-computer interaction and the extended feature greatly improves the digital operation capability of the plotting platform system. The experimental results show that the effect is improved by more than 30% compared with the traditional plotter.

1. Introduction

A plotter is a large output device used by a computer to draw graphics and pictures. Starting from

design drawing, it can be divided into vector design plotter and dotless matrix plotting. The color inkjet designer was born this year and was originally founded by Hewlett-Packard. Since the 1990s, due to the pioneering development of inkjet and print head technology, color inkjet designers have greatly improved design accuracy, color expression and reliability. Many famous designer manufacturers in the world have quickly established their own inkjet color designers. These products have the characteristics of fast design speed, low noise, large design media, good practicability and low price. They basically replaced pen designers in many fields and occupied most of the designers' market share. Consumers' awareness of color inkjet designers is also growing, and its use has expanded from the early fields to geographic information systems and other graphics and image output fields, to research, graphics, transportation and other industries. This country spends a lot of money. The ink designer equipment is imported in foreign currency. If the graphics and image production of sensitive industries such as military and geological surveys rely heavily on foreign brand manufacturers, it will create a potential crisis. Therefore, our country should have a large-format color inkjet printer designer with its own brand and technology.

Luo Sha proposed a clothing plotter system based on the integrated ARM system. ARM has the advantages of low power consumption, fast processing speed, multiple data interfaces and good real-time performance. The entire clothing plotter system that can be used to implement clothing styles, clothing design, historical records and other functions is investigated, and the design of clothing colors and popular styles in real life is introduced in detail, and the system software interface design is briefly analyzed and finally carried out. However, the software system has incomplete functions and is inconvenient to use in practice [1]. Wang Zhengwan believes that by increasing the degree of automation of clothing drawing software, the speed of drawing can be effectively increased and the workload of drawing workers can be reduced. Many modern drawing automation equipment can receive relevant drawing status information, such as coordinates, colors, frames, etc., but these systems are independent of each other and cannot exchange information, which seriously interferes with drawing efficiency. An ARM-based integrated clothing information system is proposed, which can communicate through Ethernet, exchange data between the embedded system and various subsystems, and display various information through the touch screen, and introduces the relevant hardware of the system Design and continue the detailed introduction of Ethernet communication. But his system is not running smoothly, which makes the drawing staff very distressed [2]. Xu Bin believes that ARM is a general term for microprocessors, and ARM processor is an integrated 32-bit RISC processor. Because of its unique advantages, it is widely used in embedded system design. The development of intelligent control is constantly changing us, To replace people's boring or needless work. In a life that increasingly relies on computer printing, handwritten documents can be preserved and are favored by more people. Therefore, it is necessary to design a drawing tool that imitates manuscripts. Here, we use a mobile phone application to complete the capture and analysis of text and image data, and then transfer the final coordinate data to the chip computer via Bluetooth, and then use the microchip of the chip to control the core XY structure to perform writing and drawing Features. But the algorithm is not perfect yet and needs to be improved continuously [3].

The purpose of this article is to complete the image recognition process. On this basis, an integrated hardware platform, OV2640 CMOS camera and STM32F407 and TFTLCD were created for the first time to capture, edit and display images. Then, based on the hardware platform, write and debug the corresponding code on the ARM platform, download it to the hardware platform, modify and correct according to the current state, and finally get the desired result. The integrated image processing system developed in this article can stably execute programming on a hardware

platform, and at the same time achieve the purpose of this article, which is to measure the frame rate of the received image and determine the position of the image. The dividing line and position coordinates in the picture are sent to the LCD screen for real-time display. In addition, compared with the platform with the same performance, the size of the material is relatively small, the cost is relatively low, and the code written in C language has great portability and flexibility. The system can not only meet the requirements of this article, but also can be used in other smart areas by extending some components.

2. Development Method of Clothing Plotter System

2.1. Embedded Operating System

Every embedded operating system has its advantages, disadvantages and application range. Therefore, the appropriate operating system should be selected according to different applications. Taking into account the requirements of the handheld terminal of the plotting station for the system, consider the following technical indicators:

(1) The task switching time is the time required to switch the operating system between two independent tasks with the same priority and a predefined task. The job turnaround time mainly depends on the data structure used to store the job and the scheduling algorithm adopted by the operating system. When a job is waiting or running, the current job parameters will be stored in the stack area, and the job with the highest priority will respond according to the priority of the interrupt vector table.

(2) Delayed interrupt refers to the time it takes to execute the first instruction after the interrupt signal is issued. The interrupt delay time can be divided into two parts: the maximum interrupt time and the time between interrupt processing and the execution of the first interrupt service command. In the embedded operating system, the time between the processing of the interrupt and the execution of the first interrupt service command is determined by the hardware. Therefore, the interruption delay time depends on the maximum interruption time.

(3) Deadlock release time. Usually, when two or more processes request resources to lock the resources, a deadlock occurs. The process deadlock can be solved by stopping some deadlocked processes and reallocating these resources to other deadlocked processes. Among them, the priority reversal function is an important part of solving the deadlock system. Therefore, the time taken by the operating system to resolve priority reversals largely reflects the operating system's ability to resolve deadlocks. Compared with other embedded operating systems, Linux performs well in terms of technical indicators.

In addition, embedded Linux also has the following characteristics: It has good portability, supports mainstream platforms such as x86, MIPS, ARM, etc., can choose to develop on a personal computer, and finally port to an embedded platform, saving development time; the source code is free, you can It is easy to obtain from the website; adopts modular programming ideas, easy to cut; provides complete development tools, and the powerful language compiler GCC can be easily obtained; powerful network functions, support almost all network protocols. Embedded Linux's open source, fast update speed and easy tailoring make it occupy a large share in the embedded field. Therefore, this paper chooses Linux as the embedded operating system for this subject.

2.2. Article Research Methods

The main writing methods used in this article are reference method, case study method, data

analysis method and comparison method.

(1) Reference method: search and read major related literature on advertising system development, clothing design, plotter operation steps and embedded systems under ARM in Baidu, various databases, predecessor's papers and university libraries. Obtaining specific literature information requires comprehensive knowledge and understanding of research content. In many literatures, data and evidence have been found to support the research of this article, and provide data and theoretical guidance for the research of this article.

(2) Case study method: Field investigation on the use effect of clothing plotter, understanding of the equipment of clothing plotter, in order to provide practical help for the research of this article.

(3) Data analysis method: mainly through the estimated and approximate quantitative analysis of the clothing plotter based on the ARM embedded system, to clarify the current situation and characteristics of the accuracy of big data, to find the problems in the development of high-precision data, and to Put forward strategic proposals on promotion and future development.

(4) Comparative method: Compare the ARM embedded system plotter with the traditional plotter, analyze their advantages and characteristics in the use process, so that we have a deep and comprehensive understanding of the operation steps of the plotter [13-14].

3. Development of Related Experiments Based on Arm Embedded System

3.1. Mercator Projection Algorithm

The core of the system is the STM32F407 development board, and the unit of the entire integrated imaging system is controlled by the STM32F407 chip. First, adjust the output format and resolution of the CMOS camera OV2640 through the SCCB interface. This article defines the RGB565 format with QCIF resolution (176*144). After the image is captured, the STM32F407 receives it through its own DCMI interface, and then transmits the data through DMA to define the array in this experiment, and read the TFTLCD screen, the real-time display of the table is shown in Figure 1.

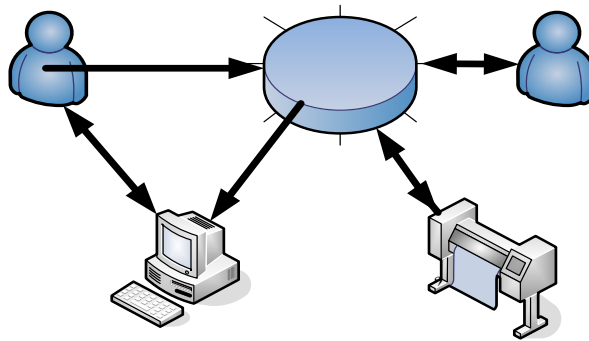


Figure 1. System structure diagram

The position of Mercator coincides with the prime meridian or the intersection of the "custom origin" and the "equator" meridian. The correct solution for the Mercator view is to convert the longitude and latitude coordinates to plane coordinates, where x is the latitude and y is the longitude. The types of positive resolution Mercator projection are as follows:

$$\begin{cases} x = r_0 q \\ y = r_0 \varphi \end{cases} \quad (1)$$

In the formula, equivalent latitude:

$$q = \ln \tan\left(\frac{\pi}{4} + \frac{\alpha}{2}\right) - \frac{e}{2} \ln 1 + e \sin \beta \quad (2)$$

Latitude circle radius of reference latitude:

$$r_0 = N_0 \cos \alpha_0 \quad (3)$$

The radius of curvature of the unitary circle at the reference latitude:

$$N_0 = A/1 - E^2 \sin \beta^2 \quad (4)$$

Path planning is to traverse all nodes according to the set search rules and find the most suitable path among them. Commonly used search strategies can be divided into two categories: exhaustive search and heuristic search. The exhaustive search verifies all the possible situations of solving the problem one by one, and finally finds the solution that meets the conditions. Exhaustive search is inefficient and consumes too much computing space and time, so exhaustive search is only suitable for solving simple problems.

3.2. Fractal Graphics of Escape Time Algorithm

The escape time algorithm has become a classic algorithm for generating fractal graphics due to its simple operation principle, less memory usage of the computer, and ability to generate high-precision graphics. The escape time algorithm is an iterative drawing method, which can generate many beautiful fractal patterns, which are rich in color, unpredictable and modern. It is an effective method of drawing fractal patterns.

$$\begin{cases} x_{t+1} = x^2 - y^2 + p \\ y_{t+1} = 2x_t y_t + q \end{cases} \quad (5)$$

Analyze the inside and outside of Julia set, showing different performance states. From the perspective of escape time algorithm, the outside of Julia set presents a divergent state, diverging to and the inside converges to a certain point or a few points, and Julia set is its escape boundary.

$$\begin{cases} x = (x_{max} - x_{min})/(a - 1) \\ y = (y_{max} - y_{min})/(b - 1) \end{cases} \quad (6)$$

For all points (x, y), x=0,1,...,a-1 and y=0,1,...,b-1 complete the following loop.

$$x_0 = x_{min} + n_x * x \quad (7)$$

According to the iterative process of formula (6), calculate (Xt, Yt) from (X1, Y1), and count t=t+1.

$$r = x_t^2 + y_t^2 \quad (8)$$

If $r > M$, select color t (t is the escape time), and go to step 5; if $t > K$, select color 0 and go to step 5; if $r > M$ and $t > K$, go to step 3.

$$z \rightarrow z^3 + c = x^3 - 3x_t + p \quad (9)$$

The escape time algorithm and complex variable function theory can derive the escape time algorithm of high-order Julia fractal graphics. Just replace the corresponding statement in the program with the following formula. The value of c is fixed, and the situation of each point (x, y) on the complex plane is recorded in the iteration. According to this rule, several Julia sets can be obtained. Changing the value of c can produce completely different Julia sets. Therefore, for the

same iterative function, there is not only the Julia set but also the Mandelbrot set. Therefore, in a sense, the Mandelbrot collection summarizes all possible Julia collections. It can be understood that the Mandelbrot collection is a very large book, and the Julia collection is just one page.

$$z \rightarrow z^4 + c = x^4 - 6x_t + p \quad (10)$$

$$z \rightarrow z^5 + c = x^5 - 10x_t + p \quad (11)$$

$$z \rightarrow z^6 + c = x^6 - 15x_t + p \quad (12)$$

Compared with the Julia set, the complexity of the Mandelbrot set belongs to a completely different category. On the one hand, the interior of the Mandelbrot set is solid without any structure, and on the other hand, its boundary is very complex, with infinitely different shapes.

$$Z_{n+1} = Z_n^2 + C, n = 0,1,2,... \quad (13)$$

In the formula, $z=(0,0)$, C is the pixel located at (p,q) on the computer screen. So the above formula becomes:

$$Z_{n+1} = (...((Z_0^2 + C)^2 + C)^2) + C \quad (14)$$

The initial value of z is set to 0, and c takes different values and repeated iterations, so that c changes regularly in the complex plane, to form an extremely complex Mandelbrot set. The Mandelbrot set records the value of c in the entire area, and the generation rule of the Julia set is to change z as the origin:

$$f(x) = f(x_0) + f'(x_0)(x - x_0) \quad (15)$$

Moving from the inside of the Mandelbrot set to its boundary. When point c reaches the boundary of the Mandelbrot set, the Julia set no longer contains any area, and has shrunk into a relatively fragile dendritic vein. When point c crosses the boundary, the Julia collection bursts open suddenly, presenting a hazy figure.

4. Design Experiment Analysis of Clothing Plotter

4.1. Fabric Performance Test and Results

The image data processing in this article is mainly realized by the difference operation of two pixels. First define one and then the array `rgb_buf[]` stores the data sent by the DCMI_DR register into this array, and then the LCD reads the data from the array `rgb_buf`, so You can complete the real-time display of the image. The process of obtaining the coordinates of the dividing line is shown in Figure 2.

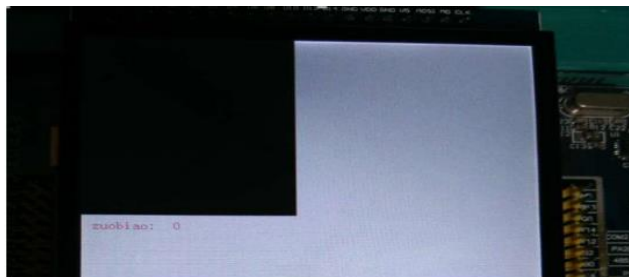


Figure 2. The absence of the boundary line

The hardware debugging of the system includes the configuration of the OV2640 CMOS camera, STM32F407 and LCD screen. Correctly connect the OV2640 CMOS camera and LCD screen to the STM32F407 according to the schematic diagram, and connect the ST-Link and USB to serial cable to the STM32F407. After powering up, download the debugged program to STM32F407, that is, the collected image can be displayed on the LCD screen. First, set the resolution of the camera to the maximum, which is UXGA (1600*1200) format. Because the screen is a 4.3-inch screen, the image will be reduced to full screen when displayed, as shown in Figure 3.



Figure 3. UXGA

In this paper, the image data collected by the OV2640 CMOS camera is sent in 8-bit, so the main control chip receives through the DCMI interface and also receives the 8-bit data broadband. The DCMI interface has a total of 14 bits D0-D13. Only the first 8 bits, D0-D7 bits, are used in this article, and the last four bits D8-D13 can be ignored. So this article needs four pixel clocks to capture a 32-bit data. The arrangement of the captured data bytes in 32-bit words is shown in Table 1.

Table 1. FAST test results of samples

Serial number	2cN/cm2 Lower thickness	Apparent thickness	Warp bending stiffness Degree B1	Weft bending Stiffness	5cN/cm negative Under the load meridian Elongation
1	0.43	0.35	0.08	8.49	5.30
2	0.24	0.21	0.03	7.66	4.01
3	0.26	0.23	0.03	8.90	5.45
4	0.18	0.15	0.03	5.38	2.39

Table 1 records the FAST test results of the sample, in which the thickness T2 under a pressure of 2cN/cm2 and the thickness T100 under a pressure of 100cN/cm2 are measured by a FAST-1 compression instrument. Among them, the apparent thickness ST is the difference between the two, which is used to characterize the compressibility of the fabric and predict the feel and appearance of the fabric. The larger the value, the softer and plump fabric; on the contrary, the fabric is smooth

and has bones. The warp bending stiffness B1 and the weft bending stiffness B2 are indirect test indicators, which are measured indirectly by the direct test indicators of the FAST-2 fabric bending tester. The longitudinal bending length C1 and the weft bending length C2 are indirectly measured. The calculation formula is: $B = W * C^3 * 9.81 * 10^{-6}$ (W is the areal density).

Table 2. FAST test results of samples

Serial number	Warp elongation under 20cN/cm load E201	Elongation E1001 in the warp direction under a load of 100cN/cm	Oblique elongation	Shear stiffness	Warp formability
1	0.97	1.63	2.73	4.90	4.86
2	0.67	1.27	2.23	3.93	4.91
3	0.83	0.27	2.97	0.90	4.51
4	0.40	1.40	1.47	4.57	4.69

Table 2 records the FAST test results of the sample. E51 and E52 are the elongation in the warp and weft directions under a load of 5 cN/cm. E201 and E202 are the elongation in the warp and weft under a load of 20cN/cm, E1001 and E1002 are the elongation in the warp and weft under a load of 100cN/cm, and EB5 is the diagonal elongation of the fabric, both of which are determined by FAST-3 fabric tensile properties. The tester is directly tested, which reflects the elongation ability of the fabric under different loads. Shear stiffness G and fabric warp and weft formability F1 and F2 are indirect test indicators.

Table 3. Fabric drape test results

Serial number	Static drape coefficient	Wave number	Uniform peak amplitude	Evenness of crest angle	Dynamic and static suspension coefficient
1	44.67	5	2.92	13.38	1.28
2	51.65	7	3.05	20.45	1.30
3	58.13	6	2.08	16.88	1.16
4	51.68	6	2.53	13.98	1.14

It can be known from the fabric drape test results in Table 3 that according to the calculation principle of the static drape coefficient, the smaller the static drape coefficient, the better the drape of the fabric, and vice versa. 3# fabric has the largest static drape coefficient, the worst drape, the fabric is stiffer, and the drape projection shape is uneven; the 1# fabric has the smallest static drape coefficient, the best drape, the fabric is softer, and the drape projection shape is uniform and natural. The comparison diagram of the two drape shapes is shown in Figure 3-2. The wave number reflects the number of flexures of the fabric in the natural drape state, which is one of the important parameters of the drape shape. Since the light and thin wool fabrics selected in this paper are all light and thin woolen fabrics, there is little difference in fabric performance.

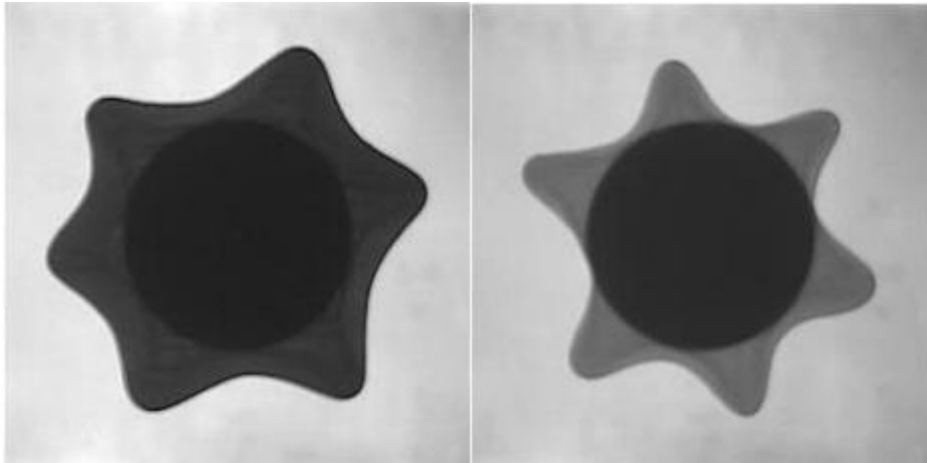


Figure 4. Comparison of drape morphology of fabric and 11# fabric

As shown in Figure 4, since the light and thin wool fabrics selected in this article, the fabric performance is not much different. From the above table, the drape wave number range of the selected samples is 5-7, and the drape wave of 1# fabric is the least. There are 5, and the number of drape waves of fabric #2 is the most, which is 7. Indexes such as uniformity of wave crest amplitude and uniformity of included angle of wave crest reflect the drape form of the fabric from different angles.

4.2. Relationship between Fabric Mechanical Properties and Miniskirt Shape

In this section, we will use factor analysis to extract the main factors of fabric performance and the main factors of miniskirt objective modeling, eliminate the lesser interference variables in the index variables, and analyze the main factors that affect fabric performance and miniskirt modeling.



Figure 5. Schematic diagram of miniskirt shape value extraction method

The image processing method is used to extract the objective evaluation indicators that reflect the shape of the miniskirt. The extracted length indicators are all the distance on the map, and the area indicators are all the area on the map. The extraction process is divided into four steps, namely, wave number index extraction, length index and angle index extraction, area index extraction and uniformity index extraction. The control position and extraction method of the miniskirt shape value are shown in Figure 5.

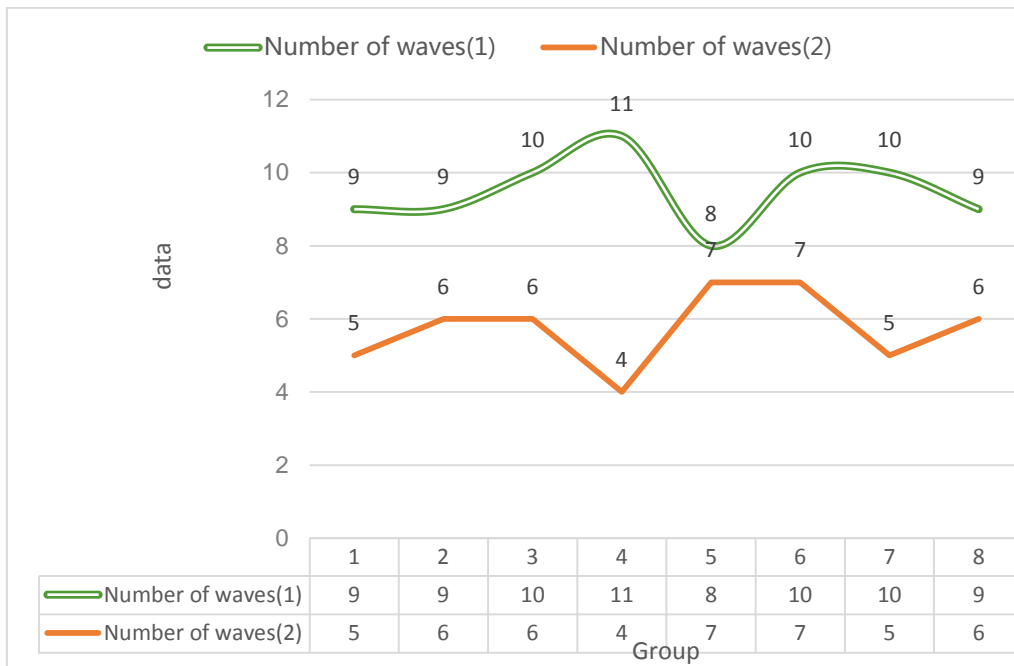


Figure 6. Wavenumber extraction results

The extraction result of the wave number index is shown in Figure 6. Wear the skirt on the platform, fix the platform base, rotate the platform 3-5 times in clockwise and counterclockwise directions, and wait for the miniskirt to reach a stable state of natural drape after it is still. When, directly read the number of peaks or valleys on the surface of the skirt, that is, the number of waves on the skirt.

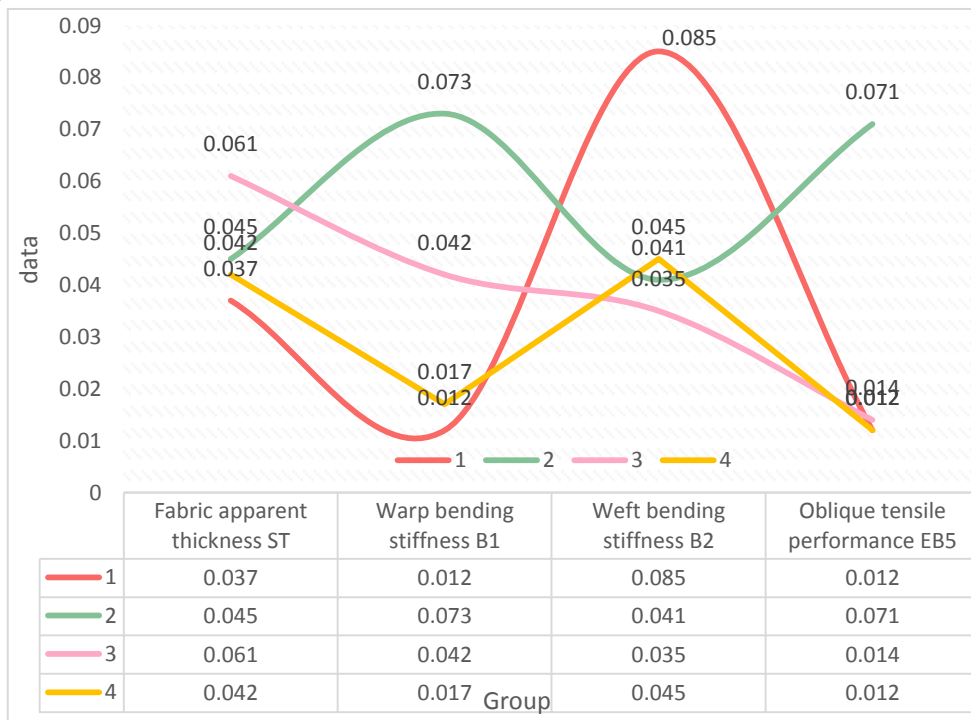


Figure 7. Fabric performance index factor analysis rotating component matrix

As shown in Figure 7, at the same time, in order to better explain the meaning of the four main factors, the paper uses the orthogonal rotation method with Kaiser standardization to obtain the result of the fabric performance index factor analysis rotation component. The drawing quality of a high-performance plotter largely depends on the positioning accuracy of the inkjet dots. For example, if the resolution of the plotter is 600dpi, then the distance between two adjacent inkjet dots is 0.0423mm, and the positioning accuracy, The requirements are very high. If the positioning is not accurate, it will cause serious defects such as thick image dots, broken lines, and blurred graphics. Therefore, the precise positioning of inkjet dots is a very critical technology. High-precision, high-performance positioning control generally adopts closed-loop servo control, but because the motor is affected by load and environmental parameters during operation, its speed change range is uncertain, and the nonlinearity of the motor speed process itself makes the traditional The PID control strategy is difficult to accurately control it, which affects the control quality and reduces the control accuracy. The following applies the human-like intelligent MFAC control strategy based on the generalized pan-model to the servo control system of the plotter. Through reasonable structural design and parameter tuning, the control quality of the system can be improved.

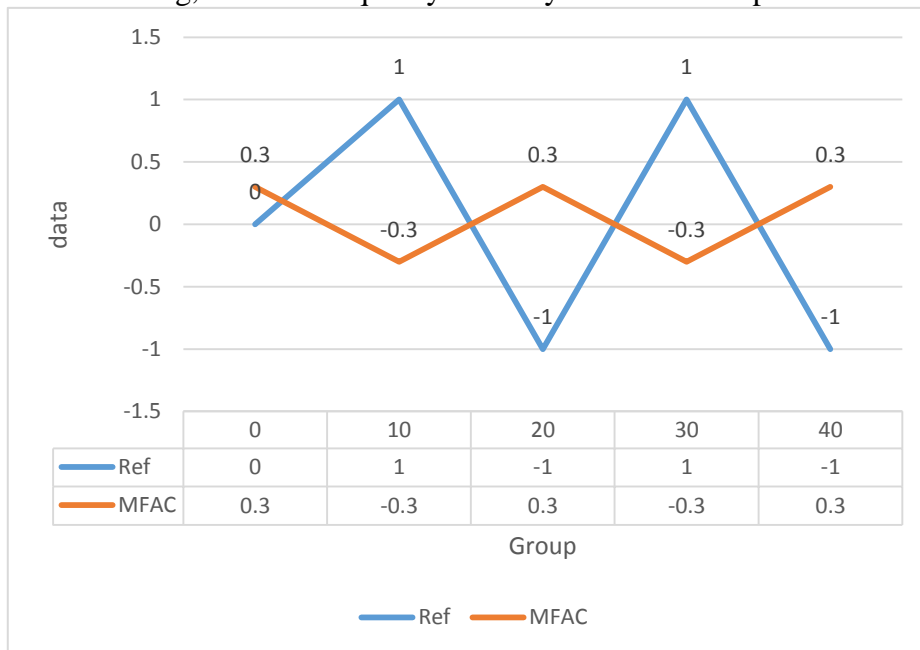


Figure 8. System output response curve under MFAC algorithm

The simulation results are shown in Figure 8. Figure 8 tracking error curve under the MFAC algorithm: It can be seen that the time-varying parameters of this system are different but the parameters used are the same, which again illustrates the wide applicability of the MFAC algorithm. Among them, T is the sampling time. At this time, the system output has no overshoot and the system response speed is fast, and the control effect is satisfactory. In the figure, there is a jump at the time of 20s due to the change of the parameters at this time, but the phase time change and the time delay time change of the system have little effect on the system, and it is not shown in the figure.

The above has realized the design of each functional module. Now design a general application program to connect the various functional modules to realize the function of the central controller as a whole. Multi-threaded design is used here. One of the reasons for using multiple threads is that it

is a very "simple" multitasking function compared to processes. We know that in the ARM system, the start of a new process must be allocated to its independent address space, and a large number of data tables must be created to handle code, batch processing and data partitioning. This is a kind of "expensive" multitasking. Multiple threads running in the computer run in the process, use the same address space, and share most of the data. The space used to start the thread is much smaller than the space required to start the process, and the switching time required for the thread is also much less, which takes longer than switching between processes. The second reason for using multiple threads is to facilitate the communication mechanism between threads. They have independent data rooms for different processes and can only transmit data through communication. This method is not only time-consuming, but also very annoying, which is not suitable for multi-threading. Since the data room is shared by threads in the same process, the data of one thread can be used directly by other threads. It is not only fast, but also very convenient. Of course, data exchange also brings other problems. Some variables cannot be changed by two threads at the same time. The data declared in some subroutines is more likely to cause catastrophic crashes in a multi-threaded program, The most important thing when writing a multi-threaded program.

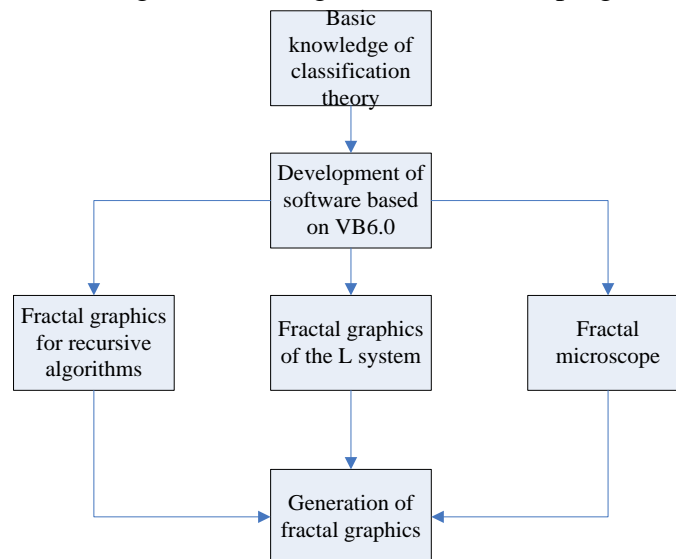


Figure 9. Program design structure diagram

The basic framework of the program design is shown in Figure 9 below. Learn to understand and master the mathematical algorithms of fractal graphics, and convert the mathematical algorithms into computer languages. This is the basis for completing the development of the fractal graphics generation system. The basic classification of fractal graphics is also necessary. This work has been completed in Chapter 2. At the same time, in order to make the obtained fractal graphics more diversified, the parameters of the fractal graphics will be set. By modifying some parameters, the shape of the graphics can be changed. Since this software is for clothing designers, it is mainly used to obtain fractal graphics. In the process of applying the obtained fractal graphics to clothing pattern design, it is necessary to use relevant clothing design software and image processing software for secondary design. Therefore, in the design of this software, functions such as color adjustment and pattern rotation are no longer provided.



Figure 10. Application effect diagram of Mandelbrot fractal graphics in clothing pattern design

As shown in Figure 10, the secondary Mandelbrot fractal graphics used here, the colors in the picture are mainly green and purple. The combination of these two colors has a certain sense of mystery. When arranging the processed graphics, the inspiration comes from the iron art-fence, The graphic shape of the unescaped area is similar to a flower, so the graphic is rotated, zoomed, and overlapped. The background color is the color in the original image, and the gradient effect comes from the color of the setting sun.

Table 4. List of coefficients for multiple regression of miniskirt modeling factor FF1 and fabric performance indicators

Model	B	Standard error	Beta	Sig
Constant	6.236	7.138	0.416	0.874
ST	-16.647	40.259	-0.332	-0.414
B1	0.055	0.298	0.116	0.185
B2	0.335	0.374	0.519	0.898

The results are shown in Table 4. Aiming at the correlation between the main factors of clothing modeling and fabric properties analyzed in this section, this section uses the method of multiple linear regression to explore the relationship between the main factors of clothing modeling and fabric properties. First, a regression analysis of the main factor FF1 of wave uniformity and fabric performance is carried out. The paper takes the fabric performance indicators closely related to the miniskirt shape including apparent thickness ST, warp and weft bending stiffness, warp and weft formability, areal density and static drape coefficient as independent variable, the main factor FF1 of wave uniformity was used as the dependent variable, and multiple linear regression was performed through SPSS software.

5. Conclusion

The embedded image processing system has a wide range of applications in engineering applications, especially the embedded image processing application based on the STM32F407 platform. The existing plotting station terminal only serves as the display device of the plotting station system, and the information is resolved. Both calculation and plotting are performed on the information processing computer, which invisibly increases the burden of the information processing computer; in addition, the lack of humanization of the terminal human-computer

interaction interface also brings inconvenience to the operation. This system designs an embedded image processing platform based on the practical application of laying waterproof coatings on smart cars. It uses STM32F407 as the main control chip to collect images through the OV2640 CMOS camera. The resolution of the collected images is configured to QCIF (176*144), the image is transmitted to the TFTLCD screen for real-time display via the DCMI interface, and the frame rate of the image acquisition is measured to be 15fps. This embedded acquisition system can meet the requirements of this experiment to a certain extent, but it also has many shortcomings. For example, the frame rate of image acquisition is relatively slow, etc. Now with the development of ARM, many high-end ARM chips such as the ARM Cortex-A series have very high clock speeds, and can be equipped with a Linux system. The resources are configured to achieve the purpose of real-time display, and the interface is also very beautiful. There are also many embedded development platforms that are built in the form of FPGA+ARM, using the high speed of FPGA parallel data processing and the control of the ARM chip to achieve more functions.

Funding

This article is not supported by any foundation.

Data Availability

Data sharing is not applicable to this article as no new data were created or analysed in this study.

Conflict of Interest

The author states that this article has no conflict of interest.

References

- [1]Luo Sha, Lu Yunjiao. *Design of ship navigation and positioning system based on ARM embedded system. Ship Science and Technology*, 2018, v.40(06):85-87.
- [2]Wang Zhengwan. *Design of ship integrated information system based on ARM embedded system. Ship Science and Technology*, 2018, v.40(14):155-157.
- [3]Xu Bin. *Discussion on ARM-based embedded system design. Science and Technology Information*, 2017, 15(028): 65-66.
- [4]Luo Yiping, Yu Jin, Qu Hongfeng. *Embedded system design based on ARM microcontroller. Equipment Maintenance Technology*, 2019, No.170(02):74-74.
- [5]Zhang Yuele, Dong Qiang. *Research on hardware design of embedded system based on ARM. Information and Computer*, 2016, 363(17):32-33.
- [6]Liu Zhendong. *Design and Implementation of Embedded Software and Hardware System Based on ARM. Information Recording Materials*, 2018, 019(004):105-106.
- [7]Lu Xinghua, Fan Tailin, Xie Zhenhan. *Multi-mode intelligent control embedded system design based on ARM. Computer and Digital Engineering*, 2016, 44(4):667-670.
- [8]Tang Hongtao. *Design of image information processing system based on ARM and embedded technology. Automation and Instrumentation*, 2016, No.198(04):42-43.
- [9]Zhang Chengfa, Li Nan. *Design and implementation of embedded Linux system based on ARM9. Shang*, 2016, 000(010):220-220.

- [10]Yin Shuihong, Li Pinghui, Yin, etc. *The design of embedded display and control system based on ARM and WinCE. Instrumentation Users*, 2017, 06(No.202): 11-14+25.
- [11]Hu Guochen. *Research on uC/OS-II embedded real-time operating system based on ARM. Information Recording Materials*, 2018, 019(012):58-60.
- [12]Zhuang Zhihui. *Design and implementation of ARM-based embedded technology course experiment system. Wireless Internet Technology*, 2017, 000(015):60-62.
- [13]Zhang Tuanshan, Wu Dewen, Zhang Chen. *Design of template sewing machine control system based on embedded Linux. Science and Technology Vision*, 2020, No.301(07):200-202.
- [14]Chen Teng. *Design and implementation of embedded display system based on i.MX6Q. Electronic Technology and Software Engineering*, 2020, 000(004): P.105-106.
- [15]Liu Peng, Feng Bo. *Embedded smart home design based on arm. Digital Communication World*, 2017, 000(010):153,165.
- [16]Huangfu Yongbing. *Digital design of shipborne radar system based on embedded technology. Ship Science and Technology*, 2018, 40(22):160-162.
- [17]*Design and Implementation of Guidance Law Simulation Platform Based on Embedded System and Virtual Reality Technology. Journal of Projectiles, Rockets, Rockets and Guidance*, 2018, v.38; No.183(02):7-12.
- [18]Wu Zongzhuo. *Design of binocular stereo vision system based on embedded Linux operating system. Electronic Testing*, 2018, 000(008): 62-63.
- [19]Lin Yuwei, Mou Sen, Jiang Haijun. *Technical practice of smart car based on ARM and embedded Linux. Computer System Applications*, 2018, v.27(08):245-250.
- [20]Dai Xiaodi, Wang Ting, DAI, et al. *Design and implementation of airborne embedded system communication based on RapidIO. Electro-Optics and Control*, 2017, 12(v.24;No.234):99-103 .
- [21]Wu Tengeng. *A design of embedded system based on DSP. Science and Technology Plaza*, 2016, 000(008): 61-63.
- [22]Han Zhuqin, Chen Shaohuang, Chen Weifeng, et al. *Design of laser marking machine based on μ COS embedded system control. Software Guide*, 2017, 016(004):124-126.
- [23]Li Xiaoyan, Xiang Liping, Xu Jian. *Research and design of embedded system experiment teaching based on project drive. Electronic World*, 2016, 000(010): 10-11.
- [24]Liang Dongquan, Wei Hong, Wei Bizhong. *Design and implementation analysis of the embedded system experiment platform based on LabVIEW. Computer Knowledge and Technology*, 2016, 12(010):253-254.
- [25]Lu Jing. *Design and implementation of image retrieval system based on embedded. Technology and Market*, 2016, 23(005):185-186.
- [26]Dong Huiwen, Yu Bicheng, Huang Haitao, et al. *Design and implementation of embedded visual tracking system. Modern Computer*, 2016, 000(016): 36-38.
- [27]Zhou Tao, Xiang Rong, Li Hao, et al. *Design and implementation of industrial control system based on embedded Linux. Electronic Design Engineering*, 2016, 24(07): 23-25.
- [28]Wang Yanchun, Luo Cangjian, Zhang Ting. *Design of Morse code reporting training system based on embedded Linux. Information and Communication*, 2016, 000(004): 55-57.
- [29]Zhou Tao, Xiang Rong, Li Hao, et al. *Design and implementation of industrial control system based on embedded Linux. Electronic Design Engineering*, 2016, 024(007): 23-25.
- [30]Li Gaojin, Fan Daren, Jiang Xingxing, et al. *Design of embedded control system for large packaging spraying based on STM32F103. Shipbuilding Technology*, 2016, 000(004): 87-93.